MINISTRY OF EDUCATION AND TRAINING
MINISTRY OF AGRICULTURE AND RURAL DEVELOPMENT

VIETNAM ACADEMY FOR WATER RESOURCES

HOANG NAM BINH

SOME HYDRODYNAMIC CHARACTERISTICS OF UNSTEADY SPATIALLY VARIED FLOW IN SIDE-CHANNEL

Specialization: **HYDRAULIC CONSTRUCTIONS ENGINEERING**

Code: **9 58 02 02**

ABSTRACT OF Ph.D DISSERTATION

HANOI - 2022

The dissertation was completed at **Vietnam Academy for Water Resources (VAWR)**

Supervisor: Prof., Dr. Le Van Nghi

Reviewer #1: Prof., Dr. Pham Ngoc Quy

Reviewer #2: Prof., Dr. Tran Dinh Hoi

Reviewer #3: Assoc. Prof. Dr. Nguyen Viet Thanh

This dissertation will be defended at the meeting of the University Doctoral Committee in Vietnam Academy for Water Resources

at............on......................., 2022

The dissertation is available at::

- The National Library;
- The Library of Vietnam Academy for Water Resources.

INTRODUCTION

1. Urgency of the dissertation

Side-channels have been interested in research since the early years of the twentieth century. The flow in the side-channel is typical with increasing discharge along the chute, also known as Spatially Variable Flow (SVF). Hydraulic regimes of side-channel flow are complicated by the air entrainment into the flow increasing the mixture flow surface close to the downstream end. The lateral flow entering the mainstream creates a strong disturbance in the flow. This generates large-scale three-dimensional (3D) spiral currents and secondary vortex, making it difficult to simulate the phenomenon mathematically and also difficult to simulate accurately.

In the current side-channel hydraulic design, the flow in the channel is considered a steady flow. The simulation equations are mainly steady one-dimensional (1D) SVF, assuming the velocity distribution is uniform, ignoring the effect of direction and force of lateral inflow. On the other hand, the flow in side-channel is essentially an unsteady SVF, and hydraulic factors have a close relationship with each other. In addition, the force of the lateral inflow makes the water level in opposite side wall consistently higher than the average water level in the side-channel; the flow is firmly mixture flow, so the velocity distribution coefficients are also different from the natural river. Therefore, the simulation results often have significant errors.

When studying 1D unsteady flow, the Saint Venant equations has solved many practical phenomena. However, when simulating for SVF in side-channel, the Saint Venant equations has not had a suitable solution because it does not have the force and energy loss of lateral flow or centrifugal force.

Based on the above discussion, the dissertation objectives are to overcome the limitation of the current method to increase accuracy by considering that the flow in the side-channel is unsteady SVF, supplementing the force of lateral flow, centrifugal force and velocity distribution coefficients. In addition, the dissertation also clarified some hydrodynamic characteristics of SVF in side-channel.

2. Objectives

(1) Propose a systems of nonlinear differential equations of 1D unsteady SVF, taking into account the force of lateral flow and the centrifugal force; (2) Discrete of the proposed equations by the finite difference method and created a computer program; (3) Determine the coefficients in the proposed equations for the side-channel; Determine some hydrodynamic characteristics in side-channel.

3. Research objects and scope of study

Research objects is open channel flow with increasing discharge along the main channel.

Scope of study is 1D flow in side-channel with increasing discharge from one side of the side-channel. The side-channel bottom slope is mild ($S_0 < S_c$), and the outflow chute bottom slope is steep ($S_0 > S_c$), the effect of air entrainment is neglected.

4. Methodology

04 main research methods were used, including: (1) Overview method to evaluate the contents related to the research; (2) Dimensional analysis to establish the experimental relationships from experimental data; (3) Mathematical analysis method to establish the 1D unsteady SVF equations by integrating the Navier - Stokes equations; (4) Numerical method to solve the proposed equations and build a computer program. In addition, the dissertation also used other methods such as survey, inheritance, and professional solutions to clarify the research contents.

5. Research contents

(1) Overview of SVF research results; (2) Study on flow characteristics in side-channel; (3) Analysis of theoretical basis and methods of creating 1D unsteady SVF differential equations; (4) Create and solve the proposed equations; (5) Determine the coefficients in the proposed equations; Create formulas to determine the opposite side wall flow depth and flow depth at the downstream end; (6) Simulation of 1D unsteady SVF and determination of some hydrodynamic characteristics of SVF in side-channel.

6. Scientific and practical significance

- Scientific significance: By adding the force of lateral flow and centrifugal force, the dissertation has established a system of differential equations for unsteady SVF, supplementing the theory for SVF. The output of the dissertation has further clarified the law of SVF and some hydrodynamic characteristics of SVF in side-channel.
- Practical significance: The dissertation has provided a side-channel hydraulic calculation program for higher accurate results than the existing method. This program allows determining the side-channel size following reality.

7. New contributions

- The research established a general form of differential equations of unsteady SVF (2.28), including the force of lateral flow and centrifugal force. Equation (2.28) is the extended form of Saint Venant's equations.
- Determined the velocity distribution coefficients of the SVF in the side-channel (α_0 = 1.41 and α = 2.32) with the application condition (3.8). Proposed the formulas to determine maximum side-channel flow depth (opposite side wall flow depth) (3.6) and flow depth at downstream end (3.17) with the application conditions (3.8) and (3.18), respectively.
- Based on the Preissmann scheme to linearize equation (2.28) to obtain a system of linear algebraic equations (2.54). Proposed an algorithm and numerical program USVF1D to determine some hydrodynamic characteristics of unsteady SVF in side-channel.

8. Dissertation outline

The dissertation has 04 main chapters, including (1) Chapter 1: Overview of research on side-channel and spatially variable flow; (2) Chapter 2: Differential equations of 1D unsteady SVF; (3) Chapter 3: Determination hydrodynamic characteristics of spatially varied flow in side-channel based on experiment data; (4) Chapter 4: Programming and apply for calculating of free-surface profiles in side-channel. In addition, the dissertation also has Introduction, Conclusion, and Appendix sections.

Chapter 1. OVERVIEW OF RESEARCH ON SIDE-CHANNEL AND SPATIALLY VARIABLE FLOW

1.1. Movement of water

The movement of water is classified in different ways. The open channel flow with increasing or decreasing discharge along the axial channel is called spatially variable flow (SVF). The SVF hydraulic regime in the side-channel is complicated by the force of the lateral inflow acting on the mainstream. 3D numerical models can simulate the hydraulic regime in the chute, but it is also difficult to describe its structure in detail. Therefore, combining simulation with physical models is necessary, but this is not always possible. Thus, it is essential to accept some assumptions to simplify the phenomenon to approximate simulation by 1D model.

1.2. Side-channel

Side-channels are typical elements of earth or rockfill dams to discharge floods sideways instead of frontally or other forms of floodway while ensuring economic and technical criteria. Some projects apply the side-channel form as follows:

- In the world: Hoover Dam (USA) is the first project to apply the side weir with a design discharge of over 10,000m^3/s based on experimental research results in the early 1930s. In addition, there are many reservoirs involving side weir such as Arrowrock, Fort Smith, Flatiron (USA), Burrinjuck, West Barwon (Australia), Karahnjukar (Iceland), Solingen, Mauer (Germany), Quelle, Rochebut (France), Townsend, Rhodeswood (England), Glendevon (Scotland), Trangslet (Sweden), Lyssbach (Switzerland), Nihotupu (New Zealand)... The side weir mentioned above is mostly ogee weir with or without spillway gates. Side-channel usually has a non-prismatic channel that gradually expands with a trapezoidal cross-section. The outflow chute is usually prismatic and has a steeper slope than the side-channel, and the bottom width is equal to the downstream end width of the side-channel.
- The projects in Vietnam are mentioned as Nuoc Ngot, Phuoc Nhon (Ninh Thuan province), My Binh, Ong Lanh, Quang Hien, Dai Son (Binh Dinh province), Dong Nghe (Da Nang city), Viet An, Loc Dai (Quang Nam province), Da Ban (Khanh Hoa province), Ong Thoai, Loc Quang, Bau Um (Binh Phuoc province), Dak Ro Ngat, Dak

Long 1 (Kon Tum province), Soc Temple (Hanoi city), Trieu Thuong 1 (Quang Tri province), Bac Khe 1 (Lang Son province), Suoi Tan 2 (Son La province). These projects are sharply crested or ogee weir applied to reservoirs with small catchment areas (under $100km^2$) without spillway gates. The spillway length is usually less than 100m, and the design discharge is less than $1000m^3/s$. The ratio between the head on weir and the spillway length ranges from 0.02 - 0.15. The chute has a non-prismatic channel that expands gradually with a trapezoidal or rectangular cross-section. The side-channel slope is about 0 - 3%. The outflow chute has a rectangular cross-section prismatic shape, and its slope is above 10%.

Projects with the same principle as side-channel, such as irrigation channels with side-weir or artificial structures (rain gutters, swimming pool overflow drain, side ditches, flow in floodplain...).

1.3. Type of 1D spatially varied flow equations

In order to generate the 1D steady SVF equation, the following assumptions are used: (1) The flow is unidirectional and ignore the cross-currents; (2) The velocity distribution is uniform; (3) The pressure in the flow is hydrostatic; (4) The effect of air entrainment is neglected; (5) The streamwise average velocity increases linearly; (6) The force of lateral inflow is neglected; (7) The flow does not appear surface waves; The Chezy - Manning formula is used to evaluate the friction loss due to the shear developed along the channel.

For SVF with increasing discharge, the equations of Hinds J. (1926), Camp T.R. (1940), Keulegan G.H. (1952), Chow V.T. (1969), Cung N.V. (1964), An H.T. (1987)... were created from the principle of conservation of momentum. The equation of Konovalov I.M. (1937) was created from the principle of conservation of energy. Flow with decreasing discharge: Chow created the equation by differentiation of the total energy head.

Hinds' equation is the first simple equation form written for steady SVF with increasing discharge.

$$\frac{dh}{dx} = \frac{v}{g}\frac{dv}{dx} + \frac{qv^2}{gQ} \tag{1.2}$$

Camp and many others developed equation (1.2) by adding the friction or velocity component of the lateral inflow and used the experimental data to determine the coefficients in this equation.

Konovalov's equation is the most general of the 1D steady SVF written for both of increasing and decreasing discharge. This equation includes the external forces of pressure, gravity, and friction and applies to the non-prismatic channel but does not yet include the force of lateral flow.

$$\frac{dh}{dx}=\frac{S_0-S_f-\frac{k_K Q}{gA^2}\frac{dQ}{dx}+\frac{\alpha Q^2}{gA^3}\frac{\partial A}{\partial x}}{1-Fr^2} \tag{1.8}$$

In the condition that the channel has a prismatic and the lateral inflow is perpendicular to the streamwise, while the velocity distribution is uniform (α = 1), then (1.8) becomes Chow's equation (1969) and if equation is written for the rectangular cross section, then (1.8) becomes the Keulegan's equation (1952).

1.4. One dimensional unsteady flow equation

For 1D unsteady flow, the classical simulation equation is known as the Saint Venant equations.

$$\frac{\partial Q}{\partial x}+\frac{\partial A}{\partial t}=q \tag{1.15}$$

$$\frac{1}{A}\frac{\partial Q}{\partial t}+\frac{1}{A}\frac{\partial}{\partial x}\left(\frac{Q^2}{A}\right)+g\frac{\partial h}{\partial x}-g\left(S_0-S_f\right)=0 \tag{1.16}$$

The basic assumptions for the analytical derivation of the Saint Venant equations are the following: (1) The flow is 1D, the water level and velocity across the section are represented by a horizontal line; (2) The fluid density is constant; (3) The streamline curvature is small, and the vertical accelerations are negligible; (4) The axial streamwise is considered as a straight centerline; (5) The bed slope is small; Sediment accretion and erosion are negligible; (6) The Manning formula is used to evaluate the friction loss due to the shear developed along the channel.

The Saint Venant equation has been applied to solve many observed phenomena with 1D hydrodynamic models such as MIKE11, HEC-RAS, ISIS (International models)... or VRSAP, KOD_01, SAL/DELTA (Domestic model)... However, the energy equation in these models has not included the force of lateral flow and the energy loss caused by the spiral currents, so it is not able to accurately solve the unsteady SVF such as flow in a side-channel.

1.5. Hydraulic researches on the side-channel

The free-surface profile is the hydraulic factor that is interested in the first and most popular research from the early 20th century to the present. The free-surface profile has many different forms, depending on the ratio of the forces and the boundary conditions. Based on experimental data, the studies shown the suitability of the 1D SVF equations, in which (1.8) has the best simulation, but it is also suitable only for the experiment for linear prismatic side-channel unaffected by local phenomena (Lucas et al., 2015). Comparison results of water surface on the physical model with a scale factor of 1:45 and original project of Karahnjukar dam, Gardarsson et al. (2015) indicated that the average water level in the physical model was lower than in the original project about 10%.

The flow pattern is very complex. The air entrainment continuously into the flow increases the mixture flow surface close to the downstream end. The spiral flow structure in the side-channel depends on the lateral inflow. The solid longitudinal vortex occurs when flow discharge or flow depth in the side-channel is small.

When the side-channel slope is mild ($S_0 < S_c$) and outflow chute slope is steep ($S_0 > S_c$), the flow depth at the downstream end (h_h) is the critical flow depth (h_c). However, the reality shows that $h_h > h_c$, according to Beij (1934), $h_h = \sqrt{3}h_c$; Kiselev (1974), $h_h = 1.1h_c$, and Nguyen Chien et al. (2004), $h_h = (1.00 - 1.33)h_c$.

According to early studies, energy loss can be neglected. However, later ones such as Mohammadi (2005), Kudzai et al. (2016) showed that the energy loss increases when the flow discharge increases along the channel and is significantly affected by the lateral inflow.

Velocity distribution: McCool's (1967) experiment showed that the SVF did not affect the velocity coefficients. Based on the theory and experimental data of Gill (1977), Kouchakzadeh et al. (2002) showed that if $\alpha_0 = 1$, the computed water level is lower than the measured data with a relatively large error. The higher the flow discharge, the stronger the impact α_0. Khiadani et al. (2012) identified the law of velocity distribution along the stream as logarithmic in both sides of the channel, the closer to the middle of the channel where impacted by the nozzle system, the velocity distribution changes to another form. In addition, on the cross section, a vortex develops from the middle towards the both sides of the channel, and a secondary vortex appears on the surface.

1.6. Conclusions for Chapter 1

SVF in the side-channel is a specific hydraulic phenomenon that many scientists have studied since the 20th century. These studies are mostly considered 1D steady flow. There are many different types of equations, but the most general and widely used is Konovalov's equation (1.8).

The flow pattern in the side-channel is complex, with the large-scale 3D spiral flow and secondary vortex. The water level along the channel and the cross-section also change very complicatedly. The velocity distribution coefficients (α and α_0) are very different from the natural river or channel. These coefficients significantly affect the water level simulation. Therefore, considering α_0 and/or $\alpha \approx 1$ will cause significant errors when computing the water level.

The types of transition from side-channel to outflow chute are also very diverse. In the case of the side-channel with mild slope ($S_0 < S_c$) and outflow chute with steep slope ($S_0 > S_c$), $h_h > h_c$, it depends on the structure and hydraulic regime.

The Saint Venant equation has been applied to solve many observed phenomena. However, with extraordinary hydraulic phenomena such as curvilinear flow or flow in a side-channel, the classical Saint Venant equation cannot be accurately solved.

In conclusion, the overview analysis in Chapter 1 shows that the unsteady SVF in general and in the side-channel, in particular, has not been thoroughly researched. In order to complete the computation method, the following chapters will create the extended Saint Venant equations for SVF, including the force of lateral flow and the centrifugal force; determine the velocity distribution, the opposite side wall flow depth, and the flow depth at the downstream end to enrich the theory of SVF, and also clarify the law of water motion in the side-channel.

Chapter 2. DIFFERENTIAL EQUATIONS OF ONE DIMENSION UNSTEADY SPATIALLY VARIED FLOW

2.1. Governing equations

Different methods can create the 1D unsteady flow equations or the Saint Venant equations. For the 1D unsteady SVF, the integration method from the Navier - Stocke's equations is used with the main forces, including gravity, friction, centrifugal, and lateral flow forces.

The basic assumptions for the analytical derivation of the 1D unsteady SVF eqs. are the following: (1) The fluid density is constant; The flow is unidirectional and ignores the cross-currents; The water level and velocity across the section is represented by a horizontal line; (2) The pressure in the gradually varied flow is hydrostatic; The velocity distribution coefficients are constant concerning time; (3) The effect of air entrainment is neglected; The flow does not appear surface waves; The vertical accelerations are negligible; (4) Sediment accretion and erosion are negligible; (5) The Manning formula is used to evaluate the friction loss due to the shear developed along the channel.

The 1D unsteady SVF eqs. has the following form:

$$\begin{cases} \dfrac{\partial Q}{\partial x} + B\dfrac{\partial Z}{\partial t} = q \\ \left(1 - Fr^2\right)\dfrac{\partial Z}{\partial x} + \dfrac{kQ}{gA^2}\dfrac{\partial Q}{\partial x} + \dfrac{k_0}{gA}\dfrac{\partial Q}{\partial t} - \dfrac{\alpha_0 BQ}{gA^2}\dfrac{\partial Z}{\partial t} - \dfrac{\alpha Q^2}{gA^3}\dfrac{\partial A}{\partial x} - \dfrac{\alpha Q^2}{gA^3}BS_0 + S_\ell = 0 \end{cases} \qquad (2.28)$$

(2.28) can be considered an extended Saint Venant's equations for an incompressible fluid, gradually varied flow, influenced by gravity, lateral flow, and centrifugal force.

If the forces of lateral flow and curvilinear flow are neglected, then $k = \alpha$, $k_0 = \alpha_0$ and $S_\ell = S_f$, (2.28) becomes the classical Saint Venant equations. If the flow is steady, the partial derivatives with respect to time are neglected, (2.28) becomes (1.8) but they have different k coefficients ($k_{K(1.8)} = 1 + \alpha - n_0$; $k_{(2.28)} = \alpha + k_\ell \alpha_0(1 - n_0)$).

2.2. Methodology of solving SVF equations

Equation (2.28) can be solved by many different methods, where the numerical method is the most suitable. The most used method in computational hydrodynamics is the finite difference method. Applying the Preissmann 4-point scheme, equation (2.28) has been transformed into linear algebraic equations containing variables.

If the side-channel is divided into N segments by (N + 1) sections (Fig. 2.24), equation (2.28) becomes equation (2.54) with 2N linear algebraic equations with 2(N + 1) Q and Z variables at $(t + \Delta t)$.

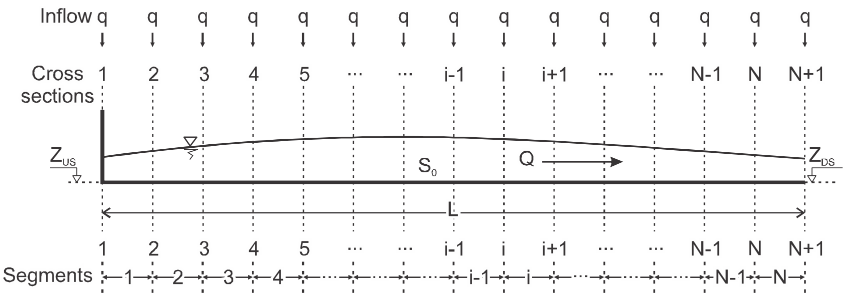

Figure 2.24. Schematic view of side-channel cross-sections

$$\begin{cases} Q_1 + (C_1)_1 Z_1 + (C_2)_1 Z_2 = (C_3)_1 & (1) \\ (C_5)_1 Z_1 + Q_2 + (C_4)_1 Z_2 = (C_6)_1 & (2) \\ Q_2 + (C_1)_2 Z_2 + (C_2)_2 Z_3 = (C_3)_2 & (3) \\ (C_5)_2 Z_2 + Q_3 + (C_4)_2 Z_3 = (C_6)_2 & (4) \\ \ldots\ldots\ldots = \ldots\ldots & \ldots \\ \ldots\ldots\ldots = \ldots\ldots & \ldots \\ Q_N + (C_1)_N Z_N + (C_2)_N Z_{N+1} = (C_3)_N & (2N-1) \\ (C_5)_N Z_N + Q_{N+1} + (C_4)_N Z_{N+1} = (C_6)_N & (2N) \end{cases} \tag{2.54}$$

(2.54) has 2N equations and 2(N + 1) unknowns therefore, it needs to be added two other equations. Those are the upstream and downstream boundary conditions, which can be (Q_1, Z_{N+1}) or (Z_1, Z_{N+1}). The recommended boundary condition to be used is equation (2.56).

$$\begin{cases} Q_1 = Q(t) \\ Z_{N+1} = Z(t) \end{cases} \tag{2.56}$$

Because the coefficients of equation (2.54) contain unknowns, an iterative method is required. For the first iteration of the time step t, the variables Q, Z are assigned in the previous step (t - 1). From the 2nd iteration onwards, the found solution gives the Q and Z variables. The iteration will stop if the computation error is less than the target error.

2.3. Conclusions for Chapter 2

The proposed equation (2.28) is created by the integration method from the Navier - Stockes equations. (2.28) is a 1D unsteady SVF equations with variable discharge along the streamwise. This is the extended Saint Venant equation, including the continuity and the energy equation, including centrifugal and lateral flow forces.

Equations (2.28) is written for 2 variables of flow discharge (Q) and water level (Z), in which the energy equation has the same form as the equation in VRSAP model. The difference between the 2 equations are the coefficient k instead of α, k_0 instead of α_0 and S_ℓ instead of S_f. The coefficients k_0, k includes coefficients of velocity distribution α_0, α, inflow ratio (k_ℓ) and velocity ratio (n_0).

Applying Preissmann 4-point scheme with weights in space and time to solve the 1D unsteady SVF equations becomes a linear algebraic equation (2.54).

If the side-channel is divided into N segments by (N + 1) sections become 2N linear algebraic equations with 2(N + 1) Q and Z variables, combining the 2 boundary conditions to form 2(N + 1) linear algebra equations. The linear algebraic equation (2.54) has the form of a 4-diagonal band matrix and is solved by the double-sweep method.

In conclusion, the main result of Chapter 2 is that the 1D unsteady SVF equations have been created. In order to close the proposed equation, it is necessary to determine some hydrodynamic characteristics of the flow in the side-channel with experimental data.

Chapter 3. DETERMINATION HYDRODYNAMIC CHARACTERISTICS OF SPATIALLY VARIED FLOW IN SIDE-CHANNEL BASED ON EXPERIMENT DATA

3.1. Physical model

The experimental reports have been collected from the VAWR, including Dong Nghe (Da Nang, Vietnam), Viet An (Quang Nam, Vietnam), and My Binh (Binh Dinh, Vietnam), the model scales are 1:30, 1:40 and 1:25, respectively. The model was designed based on the similitude criteria of Froude, and the error is within an acceptable range. Therefore, experimental data ensures reliability to use.

3.2. Flow patterns in cross-section

From the experimental reports and the article of Lucas et al. (2015), it is shown that the flow pattern on the cross-section has 1 or 2 vortexes depending on the lateral inflow and the hydraulic condition of the side-channel. The vortexes have different strengths, which form a submerged hydraulic jump. The opposite side wall flow depth (h_S) is usually higher than the other locations.

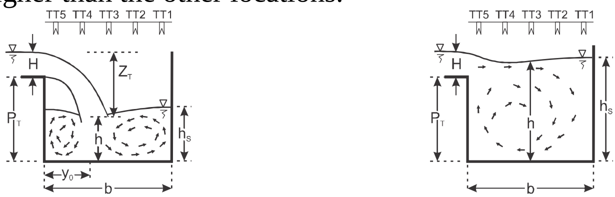

a) Free lateral inflow b) Submerged lateral inflow

Figure 3.4. Flow patterns in rectangular side-channel section

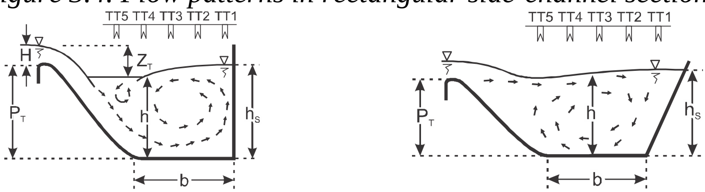

a) Free lateral inflow b) Submerged lateral inflow

Figure 3.5. Flow patterns in trapezoidal side-channel section

3.3. Opposite side wall flow depth - h_S

Experimental data at the cross-sections show that when the flow discharge changes, the ratio h_S/h also changes. In addition, this ratio tends to increase from the upstream to about 2/3 ÷ 3/4 of the downstream side-channel. This ratio increases or decreases at the downstream end depending on the hydraulic conditions upstream of the outflow chute.

By methods of variable filter and dimensional analysis, the formula (3.6) has been created to determine h_S with the application condition (3.8):

$$\frac{h_s}{h} = 1 + C_S\sqrt{\frac{q}{b\sqrt{gh}}}\left(\frac{Z_T}{h}\right)^{h/b} \tag{3.6}$$

where: C_S is the coefficient depending on the weir type; it is determined by (3.7); Other notation as shown in Figure 3.4 or 3.5.

$$\begin{cases} C_S = \bar{m} \quad (\bar{m} \text{ is mean side slope coefficient}) & \text{(for the sidechannel as shown in figure 3.5)} \\ C_S = 1 - \dfrac{y_0}{b} = 1 - \dfrac{1,33\sqrt{H(P_T + 0,3H)}}{b} & \text{(for the sidechannel as shown in figure 3.4)} \end{cases} \tag{3.7}$$

$$\left\{ \frac{Hx}{b^2} = 0,00 \div 0,50 \quad (x \text{ is streamwise coordinate}) \right. \tag{3.8}$$

Results with dependent series (My Binh) showed error within 5% (Fig. 3.12). For the independent series (Dong Nghe, Viet An), the error is mostly within 10% (Fig. 3.13). In order to improve formula reliability, (3.6) is validated by experimental series of Trangslet, Karahnjukar, Lyssbach (Lucas et al., 2015), and Markieh (Maradjieva et al., 2007).

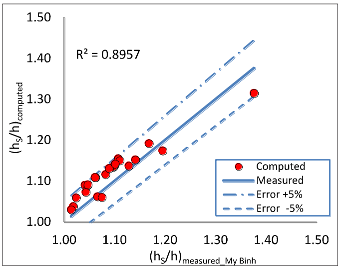

Figure 3.12. Error of the formula (3.6) for dependent data

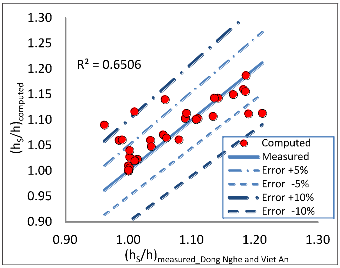

Figure 3.13. Error of the formula (3.6) for independent data

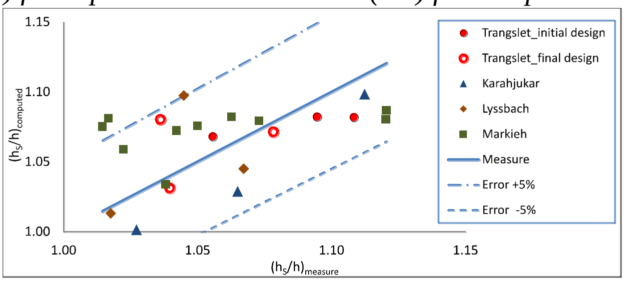

Figure 3.14. Error of the formula (3.6) for experimental data of Trangslet, Karahnjukar, Lyssbach and Markieh

Figure 3.14 shows that most of the computation results have errors within ±5.0%. Trangslet and Markieh satisfy condition (3.8) regarding the application condition, while Karahnjukar and Lyssbach do not fulfill this condition. However, more data is needed if (3.8) is extended to value 3.17 (Karahnjukar).

3.4. Velocities distribution

The mean velocity distribution on the plan view changes continuously from upstream to downstream of the side-channel and at each cross-section as the lateral inflow changes. The mainstream may appear at TT1 or TT5 and/or both sides. The velocity distribution at the end of the side-channel is close to the distribution on the outflow chute.

The vertical velocity distribution at TT1 tends to decrease from the surface to the bottom, but the difference is not significant. At TT5, this distribution is more complex, possibly reducing or vice versa. When Q and h are small, there is almost no surface flow in half of the side-channel.

The velocity distribution coefficient (α_0, α) varies in space and time, depending on hydraulic factors and project scale. The change of the coefficients α_0, α are shown in Figure 3.21 and 3.22, respectively. The mean velocity distribution coefficients are α_0 = 1.41 and α = 2.32 with the application condition (3.8).

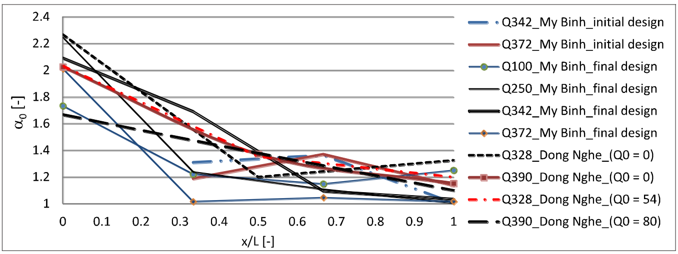

Figure 3.21. Momentum correction coefficient along the streamwise

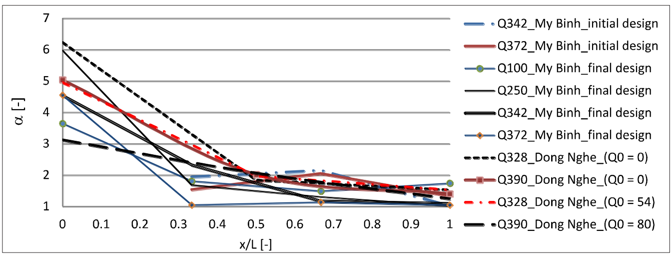

Figure 3.22. Kinetic energy correction coefficient along the streamwise

3.5. Flow depth at downstream end of side-channel - h_h

The flow depth at the downstream end (h_h) is 1 of 2 important boundary conditions when simulating hydraulic characteristics in a side-channel. When the side-channel has a mild slope ($S_0 < S_c$) and the outflow chute has a steep slope ($S_0 > S_c$), h_h can be determined according to the recommendations of Hinds, Kiselev, Beij or Chien (see section 1.5). Experimental data of Dong Nghe, Viet An, and My Binh showed that h_h also varies very complicatedly. Therefore, h_h was determined according to the previous authors is only suitable for a few cases. In order to increase the accuracy of the results, using the method of variable filter and dimensional analysis, the formula for computing h_h is created as follows: $h_h/h_{c2} = c_h^{c2} q_h^{c2}$, where: q_h = specific discharge at downstream end of side-channel ($m^3/s/m$); c_h = dimension coefficient, (s/m^2); c_2 = dimensionless coefficient. Based on experimental data of those models, these coefficients have been determined as $c_2 = 7/25$ and $c_h^{c2} = 64/125$.

$$\frac{h_h}{h_{c2}} = \frac{64}{125} q_h^{7/25} \tag{3.17}$$

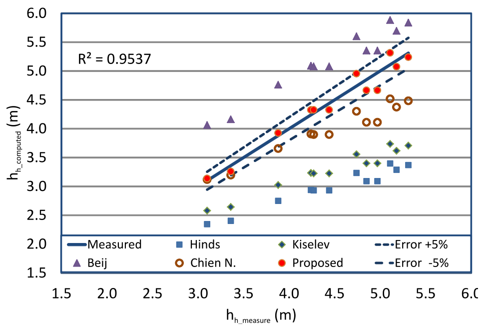

Figure 3.23. Error of the formula for flow depth at downstream end

The error of formula (3.17) is within ±5% (Fig. 3.23). The application range of formula (3.17) is:

$$\begin{cases} \dfrac{HL_{\text{weir length}}}{b_{DS}^2} = 0,11 \div 0,37 \\ \text{Side channel slope } S_0 < S_c \text{ and Outflow chute slope } S_0 > S_c. \end{cases} \tag{3.18}$$

In addition, the upper bound should be noted as follows: (1) $q_h \leq 20.5 m^3/s/m$; (2) $b \leq 38m$ (bed width of downstream end cross-section);

(3) $h_{c2} \leq 4.5$m (critical depth with $\alpha = 2.32$); (4) It is not applicable for side-channel with inflow from the first cross-section through the control structure.

Formula (3.17) needs to be independently validated to verify reliability. However, the experimental data of 3 domestic models are not enough to establish the dependent and independent series, while Trangslet, Karahnjukar, Lyssbach and Markieh models do not satisfy the 2nd application condition of (3.18). Therefore, formula (3.17) has not been independently validated. This is a limitation of this formula.

3.6. Conclusions for Chapter 3

Flow pattern on the cross section may appear 1 or 2 vortexes. The velocity distribution is very diverse, it varies from upstream to downstream end and from the weir crest sidewall to the opposite sidewall. Maximum velocity (v_{max}) does not appear in the middle of the side-channel.

The lateral inflow plunges into the side-channel, causing h_S to be generally most significant in the cross-section. h_S is determined by the formula (3.6) with the application condition (3.8).

The complexity of the velocity distribution leads to the velocity distribution coefficients varying along the streamwise and at each cross-section. The mean velocity distribution coefficients are $\alpha_0 = 1.41$ and $\alpha = 2.32$ with the application condition (3.8).

When the side-channel has $S_0 < S_c$ and the outflow chute has $S_0 > S_c$, then $h_h = h_c$ (critical depth). However, experimental data show that $h_h = (1.32 \div 1.61)h_{c1}$ (h_{c1} calculated with $\alpha = 1.00$) and $h_h = (1.01 \div 1.24)h_{c2}$ (h_{c2} calculated with $\alpha = 2.32$). h_h is determined by the proposed formula (3.17) with the application condition (3.18). The limitation of (3.17) has not been validated by independent experimental data.

In summary, equations (2.28) have been closed by velocity distribution coefficients and downstream boundary conditions by experimental data. In order to evaluate the simulation ability of (2.28) or (2.54), it is necessary to create a suitable program with a friendly interface, easy to use and display the results.

Chapter 4. PROGRAMMING AND CALCULATING FREE-SURFACE PROFILES IN SIDE-CHANNEL

4.1. USVF1D model algorithm

The 1D Unsteady Spatially Varied Flow numerical model with simulation equation (2.28) is named USVF1D. The general algorithm of USVF1D is shown in Figure 4.1.

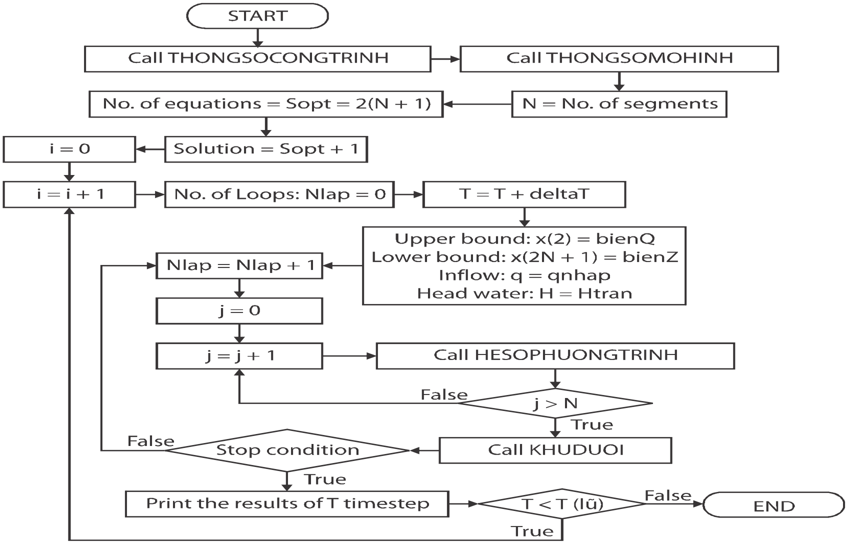

Figure 4.1. Schematic algorithm of USVF1D model

4.2. Programming

The programming tool is VBA in Microsoft Excel. The main interface of USVF1D is shown in Figure 4.8.

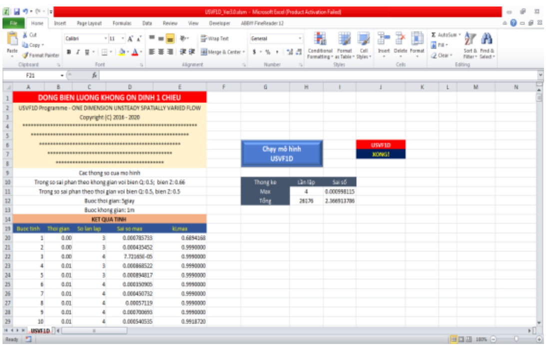


```
Sub USVF1D()
(...)
Call Thongsocongtrinh
Call Thongsomohinh
(...)
Do
    Lanlap = Lanlap + 1
    For J = 1 To m
            Call Hesophuongtrinh
    Next J
    Call Khuduoi
    Call Stopcondition
Loop Until (Saiso < 0.001)
    Call Inketqua
(...)
End Sub
```

Figure 4.8. Main sheet interface of USVF1D

4.3. Validation of USVF1D

The model is validated by experimental data of 3 domestic projects (Dong Nghe, Viet An, and My Binh). The unsteady flow over the side weir crest is established based on the experimental flow discharges. In order to be close to the experimental data in a steady flow, the flood chart is established in which $\partial Q/\partial t \approx 0$ at times corresponding to the experimental flow discharges. The side-channel is divided into segments with length Δx = 1m and time step Δt = 5s. The spatial difference weights with discharge and water level are $\eta_Q = 0.5$ and $\eta_Z = 0.66$, respectively. The results are as follows:

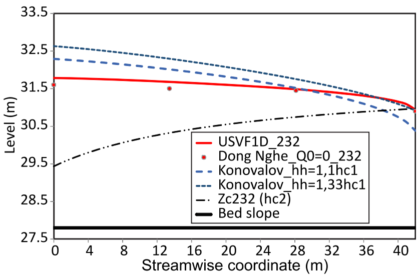

Fig 4.14. Dong Nghe free-surface profile with the scenario of closing the gate spillway for prevention of dam breaks for Q_h = 232m^3/s

Figure 4.14 note:

- USVF1D_232: free-surface profile at the time of Q_h = 232m^3/s;
- Dong Nghe_Q0=0_232: experimental water level data with Q = 232m^3/s;
- Konovalov_hh=1,1hc1: computed profile by (1.8) with $h_h = 1,1h_{c1}$, abbreviated as Kono1.1;
- Konovalov_hh=1,33hc1: computed profile by (1.8) with $h_h = 1,33h_{c1}$, abbreviated as Kono1.33;
- Zc232 (hc2): critical water level profile with α = 2,32.

Figure 4.14 shows that USVF1D is consistent with the experimental data, with 2.45% (4.57%) error. Kono1.33 is higher than Kono1.1. In 2/3 of the upstream side-channel, Kono1.1 is higher than experimental data, with a maximum error of 18.18% in the first cross-section. In 1/3 of the downstream side-channel, Kono1.1 is lower than the experimental data, with an error of 16.72%.

For Q_h = 328, 380, 390, and 410m^3/s, USVF1D is higher than experimental data, but most errors are less than 10%. Kono1.1 and Kono1.33 have 2/3 of the upstream side-channel larger than experimental data, and the downstream is lower. The overall error of Kono1.1 is larger than that of Kono1.33, and the maximum error at the upstream or downstream can exceed the range of ±30%.

For the scenario of opening spillway gate to prevent Dong Nghe dam breaks (the scenario $Q_0 > 0$), the USVF1D free-surface profile is also more consistent with the experimental data than Kono1.1 and Kono1.33. However, the flow potential energy in the side-channel has been weakened by the flow jet after the gate, so $h_h \approx h_{c2}$, causing the (3.17) to have a significant error. Therefore, it is proposed that $h_h = 1.02h_{c2}$. The computation results after adjusting the algorithm show that it is more consistent with the experimental data than the original algorithm, the error is less than 5% (Fig. 4.22, Fig. 4.23).

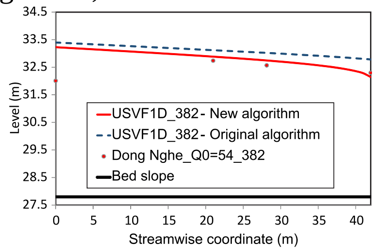

Fig. 4.22. Dong Nghe free-surface profile for the scenario $Q_0 = 54m^3/s$ for $Q_h = 382m^3/s$

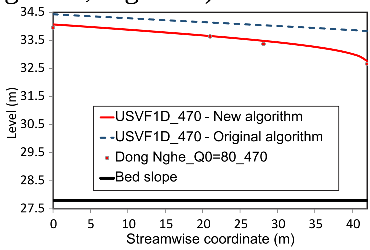

Fig. 4.23. Dong Nghe free-surface profile for the scenario $Q_0 = 80m^3/s$ for $Q_h = 470m^3/s$

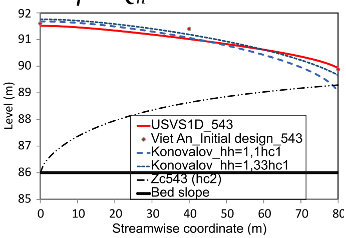

Fig. 4.25. Viet An free-surface profile for initial design for $Q_h = 543m^3/s$

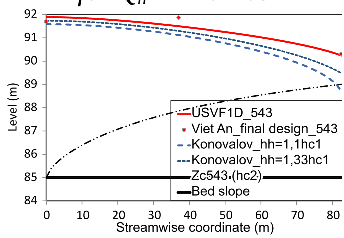

Fig. 4.26. Viet An free-surface profile for the final design for $Q_h = 543m^3/s$

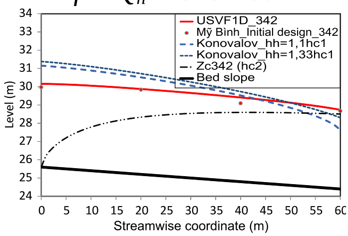

Fig. 4.28. My Binh free-surface profile for initial design for $Q_h = 342m^3/s$

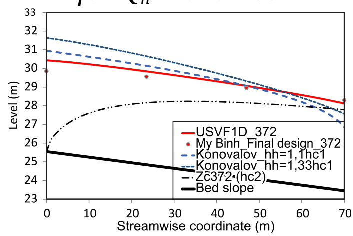

Fig. 4.28. My Binh free-surface profile for the final design for $Q_h = 372m^3/s$

For the Viet An side-channel, the USVF1D and Kono water levels at the first cross-section are consistent with experimental data. USVF1D approximates the experimental data at the downstream end, while Kono's is lower than one with an error exceeding 10% (Fig. 4.25, Fig. 4.26). For the My Binh side-channel, the computation results also show that the USVF1D in about 2/3 of the upstream side-channel is higher than the Kono and vice versa in the downstream area. Kono1.1 and Kono1.33 have large errors at the upstream and downstream (Fig. 4.28, Fig. 4.33). The overall error of USVFV1D compared with experimental data is smaller than Kono's.

The validation results of the USVF1D model show that the ability to simulate the water profile in the side-channel is more suitable than the steady SVF method. The error between the calculation and the measurement is within the acceptable range, except for the upstream area in some cases. Thus, the USVF1D model can be applied in practice.

4.4. Calculating free-surface profiles in side-channel

Applying the USVF1D model to simulate the water profile on the Trangslet, Karahnjukar, Lyssbach and Markieh side-channel. However, the outflow chute of those projects has a mild slope, so the flow depth at the downstream end is outside the application range (3.17). In the scope of study, h_h is assigned by experimental data.

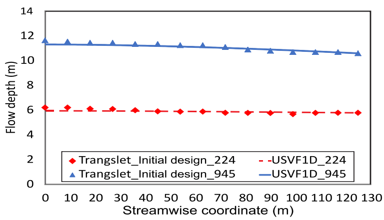

Fig 4.34. Trangslet flow depth profile for initial design

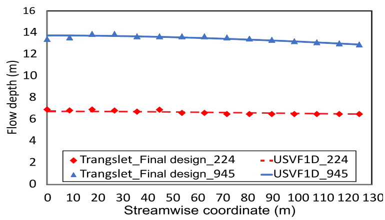

Fig 4.35. Trangslet flow depth profile for final design

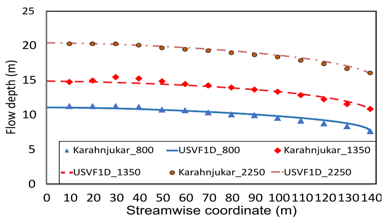

Fig 4.36. Karahnjukar flow depth profile

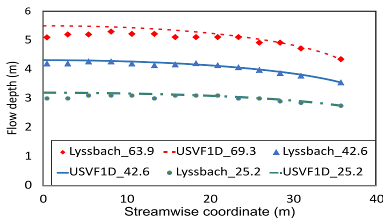

Fig 4.37. Lyssbach flow depth profile

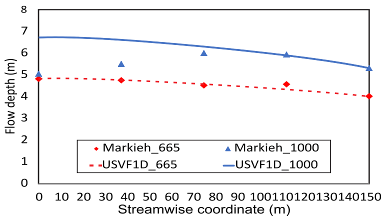

Fig 4.38. Markieh flow depth profile

Figures 4.34 to 4.38 show that the computed results are consistent with most experimental data. The computation error is within ±5%, except for the case of Markieh with Q = 1000m^3/s in the upstream area.

4.5. Conclusions for Chapter 4

The USVF1D, based on VBA language, was developed to solve the 1D unsteady SVF equations for the side-channel with lower l% iteration error. This model has an unsteady SVF computation module, allowing connection to 1D hydrodynamic models. By adding the weir module, USVF1D is able to compute unsteady SVF in the side-channel.

The USVF1D allows the user to input the parameters of side-weir, side-channel, model, and boundary conditions. The model's output is presented in tables and graphs of some hydraulic characteristics, including flow discharge, water level, flow depth and mean velocity.

The USVF1D model is validated by comparing with experimental data of 3 domestic projects (Dong Nghe, Viet An, My Binh) and 4 international projects (Trangslet, Karahnjukar, Lyssbach, Markieh). The computation results are pretty consistent with the experimental data.

By adding the inertial forces and hydrodynamic parameters of the SVF in the side-channel and considering the flow as unsteady SVF, the USVF1D model simulates the water profile more accurately than current methods.

By combining with the proposed formulas in Chapter 3, USVF1D allows the user to determine the size of the side-channel.

CONCLUSIONS AND RECOMMENDATIONS

1. Conclusions

The SVF in the side-channel is a particular case of variable mass motion. Many domestic and international scientists have studied this complex hydraulic phenomenon mainly with the assumption of 1D steady flow. Up to now, the unsteady SVF in the side-channel has not been studied. For 1D unsteady flow, there are also no studies that consider the force of the lateral flow and centrifugal force.

SVF in side-channel is one of the most complex phenomena of engineering hydraulics. The combination of horizontal and vertical flow creates vortexes in the cross-section and along the channel forming a longitudinal spiral flow. The dissertation also simulates the flow in the side-channel by 1D equations like many other authors but extends it to the unsteady flow and consider the force of the lateral flow and centrifugal force. That is the unsteady SVF equations (2.28).

The formula for computing the opposite side wall flow depth (h_S) (3.6) has been created from experimental data of 3 domestic projects with application conditions (3.8) and validated with 4 international projects. The error is within 5%.

The velocity distribution in the side-channel is very complex and is not logarithmic or exponential like other flows. Therefore, the velocity distribution coefficients α_0, α are determined by experimental data. The variation of α_0, α along the side-channel tends to decrease from the upstream to the downstream end, α_0 from 2.02 to 1.08 and α from 4.84 to 1.21, respectively. α_0 and α along the streamwise are shown in Figure 3.21 and 3.22. The mean velocity distribution coefficients are $\alpha_0 = 1.41$ and $\alpha = 2.32$ with application condition (3.8). They are used in the simulation of the water profile by equations (2.28).

The flow depth at the downstream end (h_h) is a boundary condition for computing the water profile in the side-channel. Formula (3.17) is established from experimental data of 3 domestic physical models with error within 5%, and it is applied with condition (3.18). However, (3.17) has not been independently validated because of limited experimental data.

Equations (2.28) has found an approximate solution by Preissmann 4-point scheme with spatial difference weights of water level variable η_Z and flow discharge variable η_Q, obtaining a linear algebraic equations (2.54). This is a system of 4-diagonal band matrix equations.

Equations (2.54) is used to create a program to simulate the free-surface profile in the side-channel. This program is named USVF1D, including the following modules THONGSOCONGTRINH, THONGSOMOHINH, HESOPHUONGTRINH, KHUDUOI, and many others.

USVF1D application with a time step of 5 seconds and different weights η_Z = 0.66 and η_Q = 0.50 computed the free-surface profile in the Dong Nghe, Viet An, and My Binh side-channels. The USVF1D model simulates the free-surface profile more accurately than Konovalov's method for steady SVF. Based on experimental data of Trangslet, Karahnjukar, Lyssbach, Markieh further confirmed the algorithm's correctness and the consistent velocity distribution coefficient in the side-channel.

2. Recommendations

Applying research results of the dissertation to hydraulic design of side-channel:

- Use the USVF1D model to compute the free-surface profile in the side-channel.
- Use formula (3.6) to calculate the opposite side wall flow depth and determine the level of reinforcement of the opposing sidewall to ensure financial and technical requirements.
- Apply the results of determining the velocity distribution coefficient to computed the free-surface profile in the side-channel for the steady SVF.

3. Shortcomings and further researches

a. Shortcomings and limitations

The dissertation has added centrifugal force to equations (2.28) but has not been able to evaluate the impact of this force on the flow and process the algorithm in the program USVF1D.

The experimental data of velocity distribution is not enough to determine the variation of the coefficients α_0, α along the streamwise, so the average value is accepted.

b. Further researches

The phenomenon of 1D unsteady SVF in the side-channel should be further researched and developed with the following points:

- Finalize existing problems as stated.
- The USVF1D model also needs further validation and application. In addition, it is necessary to use a 3D hydrodynamic model to compare with the results of the USVF1D model.
- Extend the application range of equations (2.28) by connecting to a river network hydraulic model to simulate flow on a river system where lateral flows are present.
- Expanding the application range of formula (3.6) to calculate h_S.
- Verify the formula (3.17) to determine the flow depth at the downstream end (h_h) in the scope of study. Extend it to other conditions.

LIST OF AUTHOR'S PUBLISHED ARTICLES

1. Hoang Nam Binh, Pham Hong Cuong, "Spatially varied flow and application in hydraulics calculation", *The Builder magazine*, p. 79-80,90, 5&6 (2017).
2. Hoang Nam Binh, "Expanding the application range of Agroskin's critical depth formula in trapezoidal open channel", *Transport and Communications Science Journal*, p. 17-23, No. 67 (2018).
3. Hoang Nam Binh, "Some remarkable study of spatially varied flow and side-channel", *Journal of Water resources science and Technology*, p. 117-124, No. 52 (2019).
4. Nguyen Vu Viet, Hoang Nam Binh, "Steady equations with increasing discharge along the channel", *The Builder magazine*, p. 58-60, No. 5&6 (2019).
5. Hoang Nam Binh, Nguyen Quoc Huy, "Establishing the Konovalov's dynamic equation for steady spatially varied flow by the principle of momentum conservation", *Vietnam Journal of Agriculture and Rural development*, p. 59-64, No. 14 (2020).
6. Hoang Nam Binh, Le Van Nghi, "Water surface profiles for steady flow with increasing discharge in a prismatic channel", *Journal of Water Resources Science and Technology*, p. 85-96, No. 68 (2021).
7. Hoang Nam Binh, Le Van Nghi, "Velocity distribution coefficients in side-channel", *Journal of Water Resources Science and Technology*, p. 89-96, No. 70 (2022).